Can Computer Vision Help Relativistic Physics? ML-JET dataset for relativistic heavy ion collisions

Anonymous CVPR submission

Paper ID

Abstract

Understanding relativistic heavy ion collision is important to study universe evolution. Traditional methods to simulate the collision reliant on Bayesian analysis which is costly and non-scalable, and deep learning has the potential to overcome it. We present a benchmark on relativistic heavy ion collisions, which simulates the relativistic heavy ion collision for about 3700 hours on a combination of GPUs and CPUs to compute many events, producing a total of 10.8 million jet event images for benchmarking relativistic heavy ion collisions. We release it to the vision community to push forward. Our dataset converts complex physics simulations into physics images, which can be compatible with standard vision classifiers. Using the standard Convolutional Neural Networks (CNN), our initial results attain a 92% accuracy in energy loss module classification, while concurrently accelerating the simulation process by an order of magnitude and saving millions of CPU/GPU hours. Our results suggest the potential of applying computer vision algorithms to physics in particle collisions discovery and beyond.

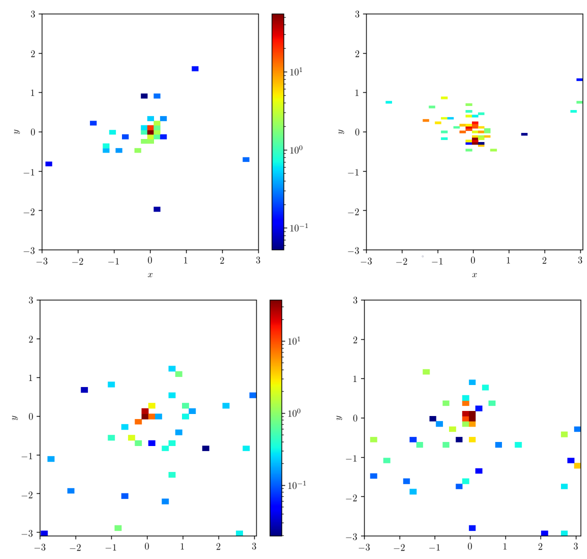

Figure 1. Representative example of Pb-Pb collision events with $Q_0 = 1.5$ and $\alpha_s = 0.2$ that show the scattering and energy of the subatomic particles, depicted as a 2D histogram. Top two figures are Matter events; bottom two figures are MATTER-LBT events. We will show how to predict the energy loss module, which is crucial for particle physics, from those events images.

1. Introduction

In the realm of high-energy heavy-ion collisions, our research addresses a crucial need —- to unravel the intricacies of the quark-gluon plasma and, specifically, to decode the elusive energy loss module within jet events. This pursuit isn't driven by mere curiosity but by the profound importance of advancing our comprehension of fundamental physics.

In the realm of relativistic heavy-ion collisions, researchers aim to investigate the Quark-Gluon Plasma (QGP) by studying jets. This pursuit involves extracting various parameters, transitioning from the abstract concept of QGP to a tangible exploration. Physicists navigate uncertainties by making assumptions about different stages, blending well-understood aspects with ambiguous segments assigned specific parameters. The ultimate goal is to precisely extract these parameters, navigating the blurred boundaries between the known and unknown in the quest to unravel the mysteries of relativistic heavy-ion collisions. Figure 2 illustrates collisions evolution in one glance.

Addressing the challenges of high-energy collisions and quark-gluon plasma intricacies [18, 28], our project takes a departure from conventional Bayesian analysis approach. Unlike the iterative simulation approach of Bayesian analysis [8], our focus is on pioneering computer vision and pattern recognition methods. Despite the success of Bayesian [12–14, 19, 36, 37], our central inquiry revolves around efficiency – can computer vision expedite the process? This

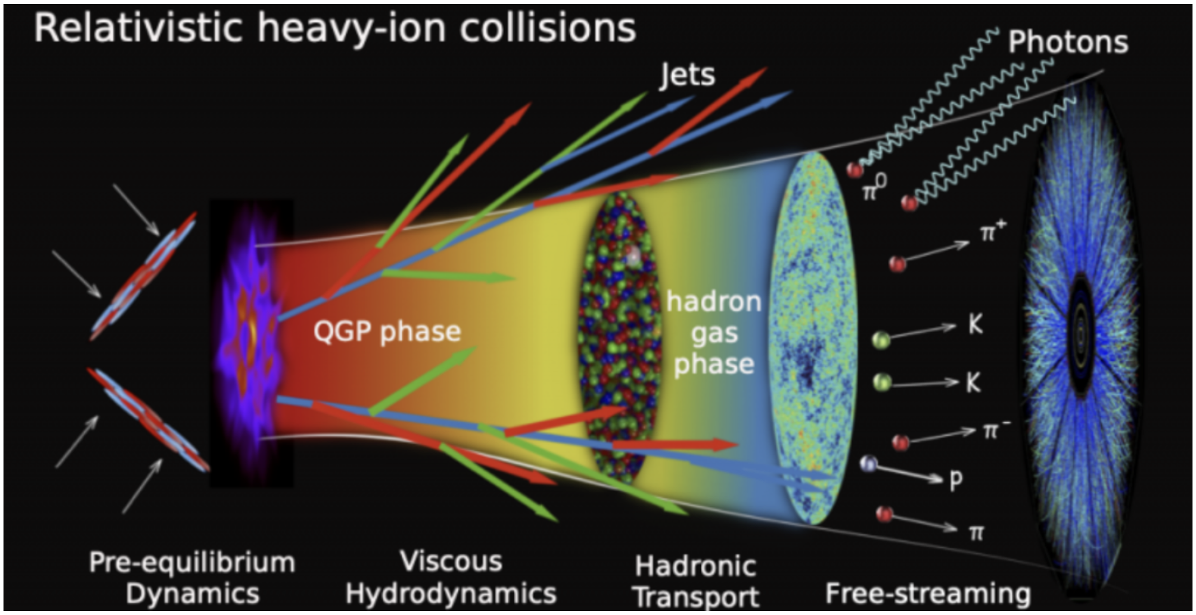

Figure 2. Relativistic heavy-ion collisions, credit to Chun Shen et. al. from JETSCAPE collaboration.

leads to our defined problem: using pattern recognition, can a ML model discern jet parameters from a set of event images? The necessity for a set of events arises due to the inadequacy of information in a single event image for comprehensive parameter analysis.

Our innovative approach centers around the ML-JET dataset, a colossal compilation of 10.8 million images exclusively designed for deep learning. Each image encapsulates crucial information, depicting three parameters: energy loss module, virtuality separation scale (Q_0), and strong coupling constant (α_s). Figure 1 illustrates for sample event collisions. The dataset's creation required an extensive 3700 hours of computational effort, utilizing significant resources —- 512 GB of memory and up to 16 CPU cores. Notably, our emphasis on energy loss module binary classification, akin to cat vs. dog classification, is crucial. This task, determining MATTER or LBT categorization, which lie at the extremes of the energy loss values, offers insights into predicting nuanced parameters. This classification initiative, our inaugural feasibility study, acts as a proof of concept for broader predictive endeavors in our research.

Utilizing state-of-art deep learning techniques, notably the VGG16 and PointNet model, we achieve unprecedented precision in classifying and analyzing energy loss modules. Rooted in a comprehensive dataset, this approach not only expands our understanding of high-energy heavy-ion collisions and the mysterious quark-gluon plasma but also represents the first in-depth examination of jet evolution within a medium. The groundbreaking result stems from the intersection of the ML-JET dataset and cutting-edge deep learning techniques, advancing our knowledge and establishing a solid foundation for a nuanced grasp of energy loss modules. Our work, with its exceptional precision, addresses gaps in prior methodologies, signifying a substantial advance in the study of high-energy collisions. The trained classifier demonstrated remarkable efficacy, boasting a 92% accuracy —- an impressive feat compared to the conventional Bayesian analysis, which is both computationally and time-consuming, lacking simultaneous consideration of all jet shower data. We will release our data, model, and code.

2. Related Work

Analyzing heavy ion collisions presents distinctive challenges, with datasets reaching gigabytes or terabytes for a limited number of design points. Unlike conventional datasets, each heavy ion collision dataset is specific to its task, creating varied samples based on governing parameters. Recent research in heavy ion collisions has addressed known issues by providing standardized datasets. While AI has been employed for jet and hydro studies, there's a notable gap in energy loss module binary classification research. Prior work focused on vacuum jets, neglecting those traversing a medium. Our research pioneers machine learning applications in examining jets within a medium, marking a significant and novel contribution to the field. [12–14, 19, 36, 37]. [9] focuses on hadron showers using ML and is specialized for specific types of hadron showers. Of these, the excellent work of [11] is most closely related, but with only four physical systems, it still lacks sufficient scale and diversity of data to challenge emerging ML algorithms.

By offering a wider, more varied problem selection and scale than these prior initiatives (18 design points with various parametrizations leading to 9 datasets), we increase the number of benchmarks available in this field. For these design aspects, we also take into account the energy loss module classification problem [7, 27] with the intention of employing ML to find latent factors that are not observable. Despite growing in prominence throughout the community, this has not yet been addressed.

One may find a summary and taxonomy of developments in heavy ion collisions in [18, 28]. Given data produced by the JETSCAPE framework [28], which itself tries to directly incorporate the tuning of parameters by Bayesian analysis, we concentrate on applying CNN models to approximate the outputs of the ground truth for creating our baselines. A range of techniques to deal with heavy ion collisions is discussed in [11, 27]. Methods include Bayesian analysis [8], principle component analysis [21], and CNN [11]. Each of these methods makes use of various presumptions, applicability domains, and data processing needs. The JETSCAPE framework is basically designed to try/understand jets moving through the medium, i.e., the Quark Gluon Plasma (QGP). Jets are localized regions of high energy traveling through the QGP. [28]

Bayesian Analysis: Although computationally expensive, Bayesian analysis is a relatively efficient means of extracting parameter values so the simulation results approximate experimental data. That's how physicists convert the problem from an abstract model to something more concrete. To make this computationally feasible, the analysis requires some assumptions about different stages/phases and considers only a subset of the available data. Some parameter values are better determined than others, and most parameter values are not independent of each other, so Bayesian analysis is used to tune the system by finding suitable parameter values. [12, 14, 19]

The Bayesian analysis research field operates by systematically varying parameters in simulations and comparing the results with real data to isolate specific parameter values. Utilizing maximum a posteriori probability (MAP), Bayesian analysis seeks the parameter space's maximum probability, reporting this as its parameter predictions. Unlike our current approach, which can determine one specific parameter at a time, Bayesian analysis aims to concurrently determine all parameter values, and its predictions depend on the interrelation of all values. [13, 36, 37]

What we are doing in the big picture and the whole idea of our research is to find a different path to determine those parameters with computer vision/pattern recognition perspective as an alternate method to Bayesian analysis.

Physicists have achieved success in utilizing Bayesian analysis to ascertain parameter values. The inquiry arises: can we enhance efficiency and speed through a computer vision approach using pattern recognition techniques? This frames the problem as follows: can a pattern recognition routine, when presented with a set of jet experimental events as images, discern the associated jet parameters? The necessity for a set of events arises from the inadequacy of information in a single event image to determine parameter values; hence, a collection of events becomes essential. In this study, as a feasibility study, we started with something simple instead of going to the last version of the problem. We started by simulating many events with some discrete values of parameters, which are determining values from the physics point of view. We then tried to see if we could train a machine to just look at the output data (event images) and recognize the original event parameters e.g., energy loss module on the predefined discrete values.

Table 1. Design point parameters leading to nine configurations that comprise the dataset

Config.	Matter Q_0	Matter-LBT Q_0	α_s	# events (in Millions)
1	1	1.5	0.2	1.2
2	1	1.5	0.3	1.2
3	1	1.5	0.4	1.2
4	1	2	0.2	1.2
5	1	2	0.3	1.2
6	1	2	0.4	1.2
7	1	2.5	0.2	1.2
8	1	2.5	0.3	1.2
9	1	2.5	0.4	1.2
				Total = 10.8

As another aspect of the big picture of the study, with Bayesian analysis, one can define parameter values and ask for a random event generator to produce events. An advantage that the machine learning-based approach would have is that it can produce these events faster, the latter methods are not highly computational/time-consuming. At the moment, with the current computational power, jet event generators e.g., JETSCAPE, take 15 minutes to generate one event, therefore it is worthwhile to explore other solutions [12, 28]. But before attempting an alternate model for jet generator, we need to make sure that we can predict the values of the parameters with pattern recognition techniques. If the outcome shows its prediction matches with real experimental data and the physics behind it with a reasonable level of uncertainty, it's proof we are on the right path toward event generators powered by AI.

We should mention that this study is just the beginning of a vast research that combines relativistic heavy ion energy physics with the pattern recognition field, and we just tried to scratch the surface. On the other hand, the Bayesian analysis approach has been a dominant approach in this field for a decade and has been well-studied already. We expect that by taking such a different approach and applying all the cutting-edge techniques in pattern recognition now available, we can develop an alternate/faster solution for the problem.

2.1. JETSCAPE

High-energy nuclear physics, specifically the study of Quark Gluon Plasma (QGP), underwent a significant shift with the introduction of heavy ion collisions at the Large Hadron Collider (LHC) [2, 3, 5, 6], marking the onset of systematic inquiry.

To cover the wide energy range from 100 GeV at the Relativistic Heavy Ion Collider (RHIC) to several TeV at the LHC, only moderate enhancements were necessary compared to existing relativistic fluid dynamical simulations of QGP evolution developed over a decade before the LHC program [15, 22, 35]. However, it became evident that an event-by-event approach was essential to compare theoretical predictions with experimental results due to the incorporation of various new physics components, including fluctuating initial states, pre-equilibrium phases, and hadronic afterburners, as depicted in Figure 5. This necessitated a sophisticated statistical framework to identify or accurately estimate numerous unknown parameters (approximately 15 for a 3+1D simulation with bulk and shear viscosity), demanding a more comprehensive simulator than previous iterations [26].

A shift in approach occurred concerning how various emissions are treated in different systems and how the medium affects jet quenching calculations. The Gyulassy-Levai-Vitev (GLV) and higher-twist methods were devised for situations with higher virtuality, where medium scattering corrected the vacuum shower, leading to a medium modified DGLAP evolution for the leading hadron's fragmentation function [17, 23, 40]. MATTER, a vacuum-like shower generator, emerged from this approach [25]. In contrast, the Baier-Dokshitzer-Mueller-Peigne-Schif (BDMPS) and Arnold-Moore-Yaffe (AMY) formalisms employ a different emission strategy.

Methods like BDMPS and AMY were designed for jets with virtuality comparable to that from multiple scattering in the medium, using Poisson emission probability or rate equation to simulate uncommon gluon releases [16, 30, 31, 38]. Approaches like Linearized Boltzmann transport (LBT)-based simulators and Q-PYTHIA incorporate mixed Monte Carlo methods at the event generator level [4, 33, 41]. JEWEL utilizes bottom-up approaches for energy loss simulation [44, 45].

Jet Energyloss Tomography with a Statistically and Computationally Advanced Program Envelope (JETSCAPE) software offers a modular architecture for event generation, advanced modules for simulating heavy ion collisions, and Bayesian statistical routines for calibration and comparison with experimental data.

Algorithm 1 ML-JET Dataset Builder Algorithm

1: Simulate nine configurations, each resulting in two final state hadron files containing 600K jet events.
2: Define jet observables: p_T, ϕ, η.
3: Define cone with radius $R = \pi$.
4: **for** each event **do**
5: Select particles satisfying $|\phi| < R$ and $|\eta| < R$.
6: Split events into 2D array.
7: Create 2D histogram with 32 bins.
8: Split plane $-\pi$ to π for $|\phi|$ and $|\eta|$ into 32×32 mesh.
9: Calculate sum of transverse momentum in each cell, $P_T = \sum_{\phi_i, \eta_i} p_{Ti}$.
10: **end for**
11: Assign energy loss module, Q_0, and α_s value as labels.
12: Divide labeled events into 90% train and 10% test data.
13: Shuffle train set for better training performance.
14: Package train and test sets into nine separate datasets.

3. ML-JET: A benchmark for relativistic heavy ion collisions

The benchmark's general learning problem is discussed in the sections that follow, along with its currently covered design points, implemented baselines (all created using Tensorflow [1]), and compliance with FAIR data standards [42].

3.1. Energy Loss in JETSCAPE

Initial parton virtuality is limited by a preset distribution and fed into the MATTER event generator. A hard parton with light-cone momentum $p^+ = (p^0 + \hat{n} \cdot \vec{p}/\sqrt{2})$ starts a virtuality-ordered shower at point r. Virtuality ($t = Q^2$) is determined using a Sudakov form factor, where α_s denotes the strong coupling constant, influencing parton scattering rates. The transport coefficient $\hat{q}$, evaluated at the scattering location, influences the splitting time of partons. Splitting functions and invariant mass differences are used to estimate daughter pair transverse momenta until parton Q^2 reaches Q_0^2.

Below Q_0^2, alternative energy loss modules like LBT may characterize the jet. Q_0 serves as the virtuality separation scale. The medium-induced gluon spectrum Γ^{inel} is calculated using the differential spectrum of radiated gluons from higher-twist energy loss formalism. Monte Carlo

Table 2. MNIST model accuracy & loss diagrams.

	$\alpha_s = 0.2$	$\alpha_s = 0.3$	$\alpha_s = 0.4$
Matter: $Q_0 = 1$, Matter-LBT: $Q_0 = 1.5$.	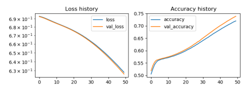	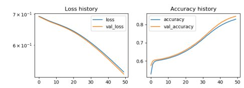	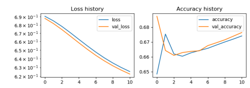
Matter: $Q_0 = 1$, Matter-LBT: $Q_0 = 2$.	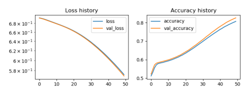	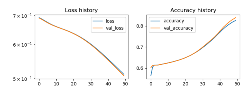	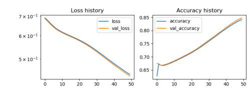
Matter: $Q_0 = 1$, Matter-LBT: $Q_0 = 2.5$.	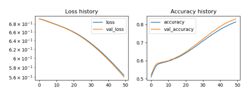	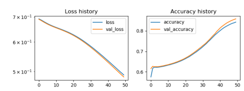	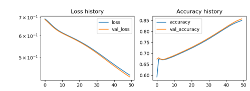

Table 3. MNIST model evaluation: accuracy

	Accuracy (%)		
	Train	Validation	Test
Config No. 1	74.12	73.87	79.58
Config No. 2	84.46	84.51	85.88
Config No. 3	68.59	68.73	68.71
Config No. 4	82.77	82.61	82.61
Config No. 5	84.04	83.93	83.95
Config No. 6	84.77	84.78	84.80
Config No. 7	83.36	83.11	83.16
Config No. 8	85.85	85.88	85.81
Config No. 9	85.64	85.68	85.61

methods determine scattering rates within a time step. This work focuses on developing a machine learning model to predict energy loss models for different Q_0 and α_s values. We explained the energy loss and its relation with $alpha_s$ and Q_0 with more quantum physics formalism details in Appendix 9

4. Data collection and pre-processing

The ML-JET dataset comprises 10.8 million 32×32 resolution images, each labeled with MATTER or MATTER-LBT associated with JET energy loss. These images are generated from simulations within the JETSCAPE framework.

To construct the dataset, jet events are generated using preset parameters in the JETSCAPE framework. Each event is pre-processed by aggregating data, clipping outliers, resizing to a standard size, converting to a 2-dimensional histogram, and normalizing pixel values. Data augmentation techniques like rotation, flipping, and cropping were unnecessary due to the dataset's ample size and variability.

Jet events simulation configuration: To construct the dataset, Pb-Pb (lead-lead) events were simulated using the JETSCAPE framework on a distributed computing Grid system. All events utilize either $Matter$ or $Matter-LBT$ as their energy loss module with a static medium.

The dataset comprises nine parts, each corresponding to different combinations of α_s and Q_0 across 18 design points. Parts with the same α_s and varying Q_0 are grouped together, resulting in nine distinct parts (see Table 1).

4.1. Matching/Filtering procedure

The algorithm 1 describes the preprocessing steps for the ML-JET dataset, including simulation, selection of relevant jet observables, creation of 2D histograms, visualization, labeling, dataset splitting, and packaging. These steps are essential for building/preparing the data for a benchmark dataset and training models in subsequent sections.Followings are jet observable used in our dataset building process:

- p_T: transverse momentum
- ϕ: azimuthal angle
- η: pseudorapidity of the emitted thermal particles

In the next section, we introduce a methodology to train models from nine datasets with 1080K training records, compile the model, and classify 120K test records and calculate the accuracy as their validation method.

5. Methodology

To predict the energy loss module, we segregate our events into either *Matter* or *Matter-LBT* labels on the basis of the features, so we are solving a binary classification problem.

We refined the predictor model's general category based on our data structure. We examined state-of-the-art pattern recognition techniques in machine learning, to solve the problem first and because jet events exhibit discernible topological structures resembling images, we opted for

Table 4. VGG16 model with 50 epochs: accuracy & loss diagrams.

	$\alpha_s = 0.2$	$\alpha_s = 0.3$	$\alpha_s = 0.4$
Matter: $Q_0 = 1$, Matter-LBT: $Q_0 = 1.5$.	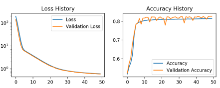	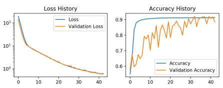	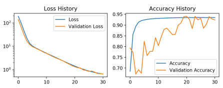
Matter: $Q_0 = 1$, Matter-LBT: $Q_0 = 2$.	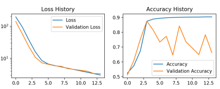	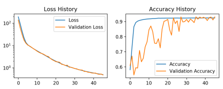	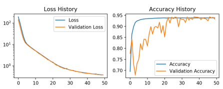
Matter: $Q_0 = 1$, Matter-LBT: $Q_0 = 2.5$.	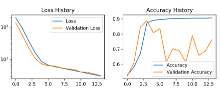	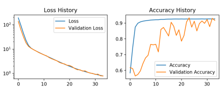	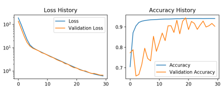

Table 5. VGG16 model with 50 epochs: accuracy.

	Accuracy (%)		
	Train	Validation	Test
Config. 1	82.58	82.65	89.98
Config. 2	92.12	92.17	92.89
Config. 3	94	94.07	93.87
Config. 4	87.45	87.54	87.26
Config. 5	93.15	93.15	93.06
Config. 6	94.34	94.3	94.29
Config. 7	88.99	88.9	88.91
Config. 8	93.24	93.3	93.24
Config. 9	94.38	94.4	94.29

computer vision and pattern recognition leading us Convolutional Neural Networks (CNN) as our next approach. Initiating our baseline models with piece-wise linear units, such as Rectified Linear Units (ReLU), we employed Adam as the optimizer.

The incorporation of Adam Batch Normalization yielded a marked improvement in optimization performance, particularly beneficial for convolutional networks and networks featuring sigmoidal nonlinearities, as evidenced by previous applications. To enhance regularization and curb overfitting, we universally implemented Early Stopping and applied Dropout as a regularizer. Furthermore, Batch Normalization was employed to minimize regularization errors effectively.

We carefully selected hyperparameters to optimize the performance of our approach. The learning rate, a critical parameter influencing the convergence of our model, was set to $[1e-1, 1e-7]$. Additionally, the architecture of our neural network was fine-tuned by specifying 4-16 hidden layers, each designed to capture intricate features relevant to our task. These hyperparameter choices were made through an iterative process of experimentation and validation, ensuring the robustness and effectiveness of our model across various scenarios. In the context of binary classification, each model employs a loss function, specifically *binary cross entropy*, consistently applied throughout our comprehensive study.

5.1. Baseline Pre-trained Models

In this section, we introduce a range of baseline models encompassing both pre-trained deep learning architectures and traditional machine learning algorithms for the energy loss module classification task. **MNIST Net** [20] and **VGG16Net** [34] serve as representatives of pre-trained deep neural network architectures. MNIST Net, initially devised for handwritten digit recognition, leverages insights into 2D shape invariances through local connection patterns and weight constraints. With 4 layers, including convolutional and fully connected layers, MNIST Net boasts 96,445 trainable parameters. On the other hand, VGG16Net, renowned for its remarkable performance in image recognition tasks, comprises 16 layers, with 4 convolutional and fully connected blocks, totaling 15,676,673 trainable parameters. **PointNet** [29] introduces a novel approach to processing point cloud data, making it uniquely suited for our jet event image classification task. Unlike conventional convolutional neural networks that operate on structured grid-like data, PointNet directly consumes unordered point sets. To ensure consistency across all models, we kept the key features of the networks such as activation function, dropout layer, optimization algorithms, loss functions, validation process, and early stopping standardized across architectures. Additionally, we include a selection of traditional machine learning algorithms:

- **Logistic Regression** serves as a fundamental binary classification algorithm that models the probability of an in-

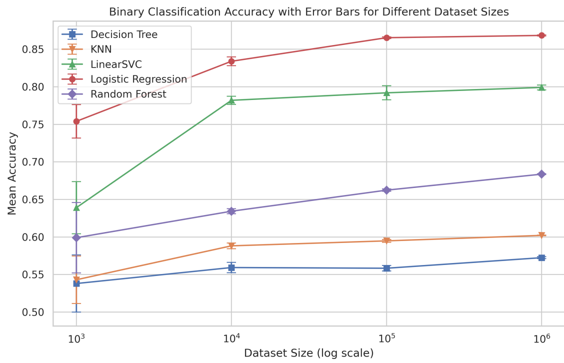

Figure 3. Trained logistic regression, decision trees, KNN, Linear SVC, and Random Forest models accuracy mean and error bar.

stance belonging to a particular class. It provides a simple yet effective baseline for comparison.

- **K-Nearest Neighbor (KNN)** is a non-parametric classification algorithm that assigns labels to instances based on the majority vote of its k-nearest neighbors in the feature space.
- **Support Vector Machine (SVM)** offers a powerful method for classification by finding the hyperplane that best separates the classes while maximizing the margin.
- **Decision Tree** constructs a tree-like model by recursively partitioning the feature space based on the feature values, making it intuitive and interpretable.
- **Random Forest** is an ensemble learning method that constructs multiple decision trees during training and outputs the mode of the classes as the prediction.

By incorporating both deep learning architectures and traditional machine learning algorithms, we facilitate a comprehensive evaluation of various models for the energy loss module classification task.

5.2. Data Format, Benchmark Access, Maintenance, and Extensibility

The benchmark consists of different data files, one for each configuration from table 1, consisting of Q_0, α_s, energy loss module label, and the event matrices, using the pickle binary data format. Each such file contains four arrays, which contain X_{train}, Y_{train}, X_{test} and Y_{test}, where each array has the dimensions N_{train}, M_{test}. N_{train} is the number of events and energy loss module labels in X_{train} and Y_{train} and M_{test} is the number events and energy loss module labels in X_{test} and Y_{test}. The scientist can leverage the predefined classes included in our benchmark code to load a particular dataset as a Tensorflow [1] dataset class. These can then be applied to create standard DataLoader instances for training unique ML models. We make use of the Hydra [43] package, which facilitates the data management and the generation of additional datasets. For the latter, we make many simulation settings available and accessible for the user to modify. As a result, users have a low entry hurdle to benchmark with fresh experiments or standard configurations.

6. Dataset analysis and evaluation

In this section, we present the outcomes of our experiments aimed at assessing the efficacy and suitability of various machine learning and deep learning methodologies on the ML-JET dataset for the task of energy loss module classification. We conducted a comprehensive analysis employing logistic regression, decision trees, K-Nearest Neighbor (KNN), Support Vector Machine (SVM), Random Forest, MNISTNet, VGG16Net, and PointNet models. Our evaluation encompasses performance metrics such as binary classification accuracy, training time, stability, and scalability across different dataset sizes. We leverage our university grid by using GPUs. We allocated 128GB memory and 32-core CPU with a GPU V100 Nvidia Tesla for training each model.

6.1. Results of Deep Learning Models

We initiated our investigation by training deep learning models, specifically Convolutional Neural Networks (CNNs), on the ML-JET dataset. Various CNN architectures, including MNIST and VGG16, were utilized with distinct configurations. Notably, the VGG16 model achieved an average accuracy of 92% on the held-out test set, showcasing its effectiveness in energy loss module classification tasks. Extensive experimentation revealed the robustness of deep learning approaches in handling complex classification problems within heavy ion physics.

We trained the MNIST model for 30 epochs, resulting in an average accuracy of 82.23% on the test data over all nine configurations. Furthermore, the VGG16 model achieved an accuracy of 88.95% for 30 epochs and 91.98% for 50 epochs. A detailed analysis of the VGG16 training on 50 epochs and MNIST, focusing on accuracy and loss diagrams for 9 different dataset configurations, is presented in Table 2 and Table 4. Respectively, we reported their detailed accuracy results in Table 3 and Table 4. The MNIST model exhibited a mean accuracy of approximately 82.78%, with error bars indicating a 95% confidence interval of $\pm 5.27\%$. This suggests a moderate level of consistency in performance. The VGG16 model trained for 30 epochs achieved a mean accuracy of 89.11%, with relatively small error bars ($\pm 2.97\%$), indicating a high degree of stability in the model's accuracy across different runs. Moreover, we explored the efficacy of PointNet models, a cutting-edge methodology tailored for point cloud data. Figure 4 demonstrates the training results of PointNet models and one sample accuracy and loss diagram for it. Our findings

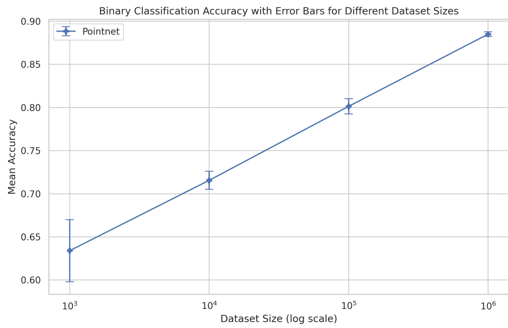

(a) Accuracy mean and error bar of trained PointNet models.

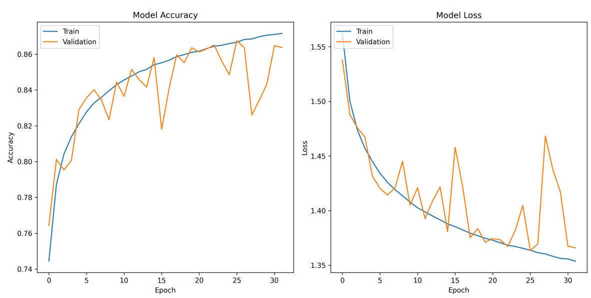

(b) Accuracy and loss of PointNet models for training and validation on a dataset size of 10^6.

Figure 4. Performance evaluation of PointNet models.

demonstrated remarkable performance, with point clouds achieving an average accuracy of approximately 88% with a dataset size of 10^6, outperforming traditional machine learning models such as logistic regression on significantly larger datasets. The trajectory of training loss across epochs exhibited consistent decrease, indicating effective learning, although vigilance against overfitting was warranted.

6.2. Results of Machine Learning Models

In parallel, we evaluated traditional machine learning models including logistic regression, decision trees, KNN, Linear SVC, and Random Forest. Logistic regression emerged as a strong contender, achieving an average accuracy of approximately 87%, surpassing other traditional models in the context of energy loss module classification. However, the accuracy plateaued around 87% even with increased dataset sizes, suggesting the necessity for alternative approaches, particularly in scenarios demanding higher accuracy.

Linear SVC, Random Forest, KNN, and Decision Tree techniques followed, demonstrating varying degrees of performance. While Linear SVC exhibited a plateauing trend in accuracy around 80%, Random Forest showcased a linear increase with dataset size expansion. Nevertheless, extrapolation indicated substantial dataset size requirements to match logistic regression accuracy levels. KNN and Random Forest displayed incremental accuracy improvements up to a certain dataset size, indicating their efficacy for moderate-scale datasets.

7. Conclusion

In this paper, we presented a new dataset named ML-JET that is specifically designed for deep learning applications. The dataset consists of 10.8 million images with a resolution of 32×32, each associated with energy loss module labels (Matter and Matter-LBT). We believe that this dataset is valuable to researchers and practitioners in the field of deep learning and phenomenal physics, enabling them to develop and test new models for various tasks such as medium parameter classification and event parameter prediction. We will release the dataset publicly to allow others to replicate our experiments and build upon our findings. Furthermore, our study underscores the efficacy of both deep learning and traditional machine learning methodologies in addressing energy loss module classification tasks. While deep learning models, particularly VGG16 and PointNet, demonstrated superior accuracy and scalability, traditional machine learning approaches, especially logistic regression, remain viable options, particularly in resource-constrained environments. For the specific requirements of the application and the available computational resources, we recommend pattern recognition techniques using deep neural networks.

8. Discussion and Future Studies

After successfully building a novel dataset of jet events and using it to classify the energy loss module in this study, we plan to extend the study by leveraging the dataset for more machine learning and deep learning tasks. Some possible future studies include the following:

- Develop and train deep models individually for classifying and predicting the α_s and Q_0 values.
- Construct a synthesis deep model to simultaneously predict the energy loss module, α_s, and Q_0 values.
- Create an application capable of extracting all environmental parameters associated with each event from event images.
- Expand the dataset from a static medium to a hydrodynamic medium, generate/simulate events, and build a dataset with the hydrodynamic profile.
- Develop and train deep models for the expanded dataset.
- Conduct a comparative analysis between the resulting models.

We encourage fellow scientists in the field to utilize the ML-JET dataset to explore additional mysteries of the universe.

References

[1] Martín Abadi, Ashish Agarwal, Paul Barham, Eugene Brevdo, Zhifeng Chen, Craig Citro, Greg S. Corrado, Andy Davis, Jeffrey Dean, Matthieu Devin, Sanjay Ghemawat, Ian Goodfellow, Andrew Harp, Geoffrey Irving, Michael Isard, Yangqing Jia, Rafal Jozefowicz, Lukasz Kaiser, Manjunath Kudlur, Josh Levenberg, Dandelion Mané, Rajat Monga, Sherry Moore, Derek Murray, Chris Olah, Mike Schuster, Jonathon Shlens, Benoit Steiner, Ilya Sutskever, Kunal Talwar, Paul Tucker, Vincent Vanhoucke, Vijay Vasudevan, Fernanda Viégas, Oriol Vinyals, Pete Warden, Martin Wattenberg, Martin Wicke, Yuan Yu, and Xiaoqiang Zheng. TensorFlow: Large-scale machine learning on heterogeneous systems, 2015. Software available from tensorflow.org. 4, 7

[2] John Adams, MM Aggarwal, Z Ahammed, J Amonett, BD Anderson, D Arkhipkin, GS Averichev, SK Badyal, Y Bai, J Balewski, et al. Experimental and theoretical challenges in the search for the quark–gluon plasma: The star collaboration's critical assessment of the evidence from rhic collisions. *Nuclear Physics A*, 757(1-2):102–183, 2005. 4

[3] K Adcox, SS Adler, S Afanasiev, C Aidala, NN Ajitanand, Y Akiba, A Al-Jamel, J Alexander, R Amirikas, K Aoki, et al. Formation of dense partonic matter in relativistic nucleus–nucleus collisions at rhic: experimental evaluation by the phenix collaboration. *Nuclear Physics A*, 757(1-2):184–283, 2005. 4

[4] Nestor Armesto, Leticia Cunqueiro, and Carlos A Salgado. Q-pythia: a medium-modified implementation of final state radiation. *The European Physical Journal C*, 63:679–690, 2009. 4

[5] I Arsene, IG Bearden, D Beavis, C Besliu, B Budick, H Bøggild, C Chasman, CH Christensen, P Christiansen, J Cibor, et al. Quark–gluon plasma and color glass condensate at rhic? the perspective from the brahms experiment. *Nuclear Physics A*, 757(1-2):1–27, 2005. 4

[6] BB Back, MD Baker, M Ballintijn, DS Barton, B Becker, RR Betts, AA Bickley, R Bindel, A Budzanowski, W Busza, et al. The phobos perspective on discoveries at rhic. *Nuclear Physics A*, 757(1-2):28–101, 2005. 4

[7] Austin A Baty. *Study of parton energy loss in heavy ion collisions using charged particle spectra measured with CMS*. PhD thesis, Massachusetts Institute of Technology, 2019. 3

[8] Jonah E Bernhard, J Scott Moreland, Steffen A Bass, Jia Liu, and Ulrich Heinz. Applying bayesian parameter estimation to relativistic heavy-ion collisions: simultaneous characterization of the initial state and quark-gluon plasma medium. *Physical Review C*, 94(2):024907, 2016. 1, 3

[9] Erik Buhmann, Sascha Diefenbacher, Daniel Hundhausen, Gregor Kasieczka, William Korcari, Engin Eren, Frank Gaede, Katja Krüger, Peter McKeown, and Lennart Rustige. Hadrons, better, faster, stronger. *Machine Learning: Science and Technology*, 3(2):025014, 2022. 2

[10] Shanshan Cao and Abhijit Majumder. Nuclear modification of leading hadrons and jets within a virtuality ordered parton shower. *Physical Review C*, 101(2):024903, 2020. 1

[11] Yi-Lun Du, Daniel Pablos, and Konrad Tywoniuk. Deep learning jet modifications in heavy-ion collisions. *Journal of High Energy Physics*, 2021(3):1–50, 2021. 2, 3

[12] R Ehlers, A Angerami, R Arora, SA Bass, S Cao, Y Chen, L Du, T Dai, H Elfner, W Fan, et al. Bayesian analysis of qgp jet transport using multi-scale modeling applied to inclusive hadron and reconstructed jet data. *arXiv preprint arXiv:2208.07950*, 2022. 1, 2, 3

[13] D Everett, D Oliinychenko, M Luzum, J-F Paquet, G Vujanovic, SA Bass, L Du, C Gale, M Heffernan, U Heinz, et al. Role of bulk viscosity in deuteron production in ultrarelativistic nuclear collisions. *Physical Review C*, 106(6):064901, 2022. 3

[14] W Fan, G Vujanovic, SA Bass, A Majumder, A Angerami, R Arora, S Cao, Y Chen, T Dai, L Du, et al. Multi-scale evolution of charmed particles in a nuclear medium. arxiv 2022. *arXiv preprint arXiv:2208.00983*, 2022. 1, 2, 3

[15] Charles Gale, Sangyong Jeon, Björn Schenke, Prithwish Tribedy, and Raju Venugopalan. Event-by-event anisotropic flow in heavy-ion collisions from combined yang-mills and viscous fluid dynamics. *Physical review letters*, 110(1):012302, 2013. 4

[16] Sangyong Jeon and Guy D Moore. Energy loss of leading partons in a thermal qcd medium. *Physical Review C*, 71(3):034901, 2005. 4

[17] Zhong-Bo Kang, Robin Lashof-Regas, Grigory Ovanesyan, Philip Saad, and Ivan Vitev. Jet quenching phenomenology from soft-collinear effective theory with glauber gluons. *Physical Review Letters*, 114(9):092002, 2015. 4

[18] A Kumar, Y Tachibana, D Pablos, C Sirimanna, RJ Fries, A Majumder, A Angerami, SA Bass, S Cao, Y Chen, et al. Jetscape framework: p+ p results. *Physical Review C*, 102(5):054906, 2020. 1, 3

[19] A Kumar, Y Tachibana, C Sirimanna, G Vujanovic, S Cao, A Majumder, Y Chen, L Du, R Ehlers, D Everett, et al. Inclusive jet and hadron suppression in a multistage approach. *Physical Review C*, 107(3):034911, 2023. 1, 2, 3

[20] Yann LeCun, Léon Bottou, Yoshua Bengio, and Patrick Haffner. Gradient-based learning applied to document recognition. *Proceedings of the IEEE*, 86(11):2278–2324, 1998. 6

[21] Ziming Liu, Wenbin Zhao, and Huichao Song. Principal component analysis of collective flow in relativistic heavy-ion collisions. *The European Physical Journal C*, 79(10):870, 2019. 3

[22] Matthew Luzum and Paul Romatschke. Viscous hydrodynamic predictions for nuclear collisions at the lhc. *Physical review letters*, 103(26):262302, 2009. 4

[23] A Majumder. The in-medium scale evolution in jet modification. *arXiv preprint arXiv:0901.4516*, 2009. 4

[24] Abhijit Majumder. Hard collinear gluon radiation and multiple scattering in a medium. *Physical Review D*, 85(1):014023, 2012. 1

[25] Abhijit Majumder. Incorporating space-time within medium-modified jet-event generators. *Physical Review C*, 88(1):014909, 2013. 4

[26] John Novak, Kevin Novak, Scott Pratt, Joshua Vredevoogd, CE Coleman-Smith, and RL Wolpert. Determining funda-

mental properties of matter created in ultrarelativistic heavy-ion collisions. *Physical Review C*, 89(3):034917, 2014. 4

[27] Long-Gang Pang. Machine learning for high energy heavy ion collisions. *Nuclear Physics A*, 1005:121972, 2021. 3

[28] JH Putschke, K Kauder, E Khalaj, A Angerami, SA Bass, S Cao, J Coleman, L Cunqueiro, T Dai, L Du, et al. The jetscape framework. *arXiv preprint arXiv:1903.07706*, 2019. 1, 3

[29] Charles R Qi, Hao Su, Kaichun Mo, and Leonidas J Guibas. Pointnet: Deep learning on point sets for 3d classification and segmentation. In *Proceedings of the IEEE conference on computer vision and pattern recognition*, pages 652–660, 2017. 6, 4

[30] Guang-You Qin, Joerg Ruppert, Charles Gale, Sangyong Jeon, and Guy D Moore. Jet energy loss, photon production, and photon-hadron correlations at energies available at the bnl relativistic heavy ion collider (rhic). *Physical Review C*, 80(5):054909, 2009. 4

[31] Carlos A Salgado and Urs Achim Wiedemann. Calculating quenching weights. *Physical Review D*, 68(1):014008, 2003. 4

[32] L Santos, GV Shlyapnikov, P Zoller, and M Lewenstein. Bose-einstein condensation in trapped dipolar gases. *Physical Review Letters*, 85(9):1791, 2000. 1

[33] B Shim, G Hays, R Zgadzaj, T Ditmire, and MC Downer. Enhanced harmonic generation from expanding clusters. *Physical review letters*, 98(12):123902, 2007. 4

[34] Karen Simonyan and Andrew Zisserman. Very deep convolutional networks for large-scale image recognition. *arXiv preprint arXiv:1409.1556*, 2014. 6

[35] Huichao Song, Steffen A Bass, Ulrich Heinz, Tetsufumi Hirano, and Chun Shen. 200 a gev au+ au collisions serve a nearly perfect quark-gluon liquid. *Physical Review Letters*, 106(19):192301, 2011. 4

[36] Y Tachibana, A Angerami, R Arora, SA Bass, S Cao, Y Chen, T Dai, L Du, R Ehlers, H Elfner, et al. Comprehensive study of multi-scale jet-medium interaction. *arXiv preprint arXiv:2212.12188*, 2022. 1, 2, 3

[37] Y Tachibana, A Kumar, A Majumder, A Angerami, R Arora, SA Bass, S Cao, Y Chen, T Dai, L Du, et al. Hard jet substructure in a multi-stage approach. *arXiv preprint arXiv:2301.02485*, 2023. 1, 2, 3

[38] Simon Turbide, Charles Gale, Sangyong Jeon, and Guy D Moore. Energy loss of leading hadrons and direct photon production in evolving quark-gluon plasma. *Physical Review C*, 72(1):014906, 2005. 4

[39] Enke Wang. Heavy quark energy loss in a nuclear medium. *Physical Review Letters*, 93, 2004. 1

[40] Xin-Nian Wang and Xiaofeng Guo. Multiple parton scattering in nuclei: Parton energy loss. *Nuclear Physics A*, 696 (3-4):788–832, 2001. 4

[41] Yongjia Wang, Chenchen Guo, Qingfeng Li, Zhuxia Li, Jun Su, and Hongfei Zhang. Influence of differential elastic nucleon-nucleon cross section on stopping and collective flow in heavy-ion collisions at intermediate energies. *Physical Review C*, 94(2):024608, 2016. 4

[42] Mark D Wilkinson, Michel Dumontier, IJsbrand Jan Aalbersberg, Gabrielle Appleton, Myles Axton, Arie Baak, Niklas Blomberg, Jan-Willem Boiten, Luiz Bonino da Silva Santos, Philip E Bourne, et al. The fair guiding principles for scientific data management and stewardship. *Scientific data*, 3(1):1–9, 2016. 4

[43] Omry Yadan. Hydra-a framework for elegantly configuring complex applications. *Github*, 2:5, 2019. 7

[44] Korinna Zapp, Johanna Stachel, and Urs Achim Wiedemann. Local monte carlo implementation of the non-abelian landau-pomeranchuk-migdal effect. *Physical review letters*, 103(15):152302, 2009. 4

[45] Korinna C Zapp, Frank Krauss, and Urs A Wiedemann. A perturbative framework for jet quenching. *Journal of high energy physics*, 2013(3):1–33, 2013. 4

Can Computer Vision Help Relativistic Physics? ML-JET dataset for relativistic heavy ion collisions

Supplementary Material

9. Energy Loss Module Phycics Formalism

The initial virtuality of the partons will have a maximum limit set by the preset distribution. These will then be introduced into the MATTER event generator. In MATTER, a single hard parton created at a point r with a forward light-cone momentum $p^+ = (p^0 + \hat{n} \cdot \vec{p}/\sqrt{2})$ where $\hat{n} = \vec{p}/|\vec{p}|$ starts a virtuality-ordered shower.
To ascertain the real virtuality ($t = Q^2$) of the given parton, one may sample a Sudakov form factor,

$$\Delta(t, t_0) = \exp\left[- \int_{t_0}^{t} \frac{dQ^2}{Q^2} \frac{\alpha_s(Q^2)}{2\pi} \int_{t_0/t}^{1-t_0/t} dz P(z) \right. \\ \left. \times \left\{ 1 + \int_0^{\zeta + MAX^+} d\zeta^+ \frac{\hat{q}(r+\zeta)}{Q^2(1-z)} \Phi(Q^2, p^+, \zeta^+) \right\} \right], \tag{1}$$

where Φ represents a sum over phase factors that depends on ζ^+, p^+, and Q. The transport coefficient $\hat{q}$ is evaluated at the location of scattering $\vec{r} + \hat{n}\zeta^+$, $P(z)$ is the vacuum splitting function, and $\zeta_M AX^+$ is the maximum length ($1.2\tau_f^+$), which is used to sample the actual splitting time of the given parton with τ_f^+ as the mean light-cone formation time $\tau_f^+ = 2p^+/Q^2$ [10]. After determining Q^2, z can be sampled using the splitting function $P(z)$. The transverse momentum of the created daughter pair can be estimated using the difference in invariant mass between the parent and daughters. This method is repeated until a given parton's Q^2 reaches a specific value for Q_0^2.
Below Q_0^2 the jet might be better characterized by another energy loss module such as LBT, which can evolve according to the linear Boltzmann equation. Q_0 is the virtuality separation scale. For our dataset, the medium-induced gluon spectrum

$$\Gamma^{inel} = \int dx dk_\perp^2 \frac{dN_g}{dx dk_\perp^2 dt}, \tag{2}$$

where the differential spectrum of radiated gluon is taken from the higher-twist energy loss formalism [24, 32, 39]:

$$\frac{dN_g}{dx dk_\perp^2 dt} = \frac{2\alpha_s C_A \hat{q} P(x) k_\perp^4}{\pi(k_\perp^2 + x^2 m^2)^4} \sin^2\left(\frac{t - t_i}{2\tau_f}\right), \tag{3}$$

where x and $k_\perp$ are the fractional energy and transverse momentum of the emitted gluon with respect to its parent parton, α_s is the strong coupling constant, $C_A = N_c$ is the gluon color factor, $P(x)$ is the splitting function, $\hat{q}$ is the transport coefficient, t_i denotes the production time of the given parton, and $\tau_f = 2Ex(1-x)/k_\perp^2 + x^2m^2$ is the formation time of the radiated gluon with E and m as the parton energy and mass, respectively. With these scattering rates, the Monte Carlo method is applied to determine whether scattering happens within a given time step. In this work, we develop a ML model to determine the energy loss model for different values of Q_0 and α_s.

10. Heavy Ion Collisions

In this section, we show a visualization that depicts the multi-stage approach that is leveraged in the JETSCAPE for jet evolution in Figure 5.

11. Sample events

In this appendix, we provide sample events for configurations two through nine of the dataset, depicted in Figures 6 through 23.

12. Calculating Accuracy for VGG16 Training for 50 epoch Config. #9 - Test Data

One of the methods for assessing classification models is accuracy, which is simply the percentage of correct predictions. For binary classification, accuracy can also be calculated in terms of positives and negatives as in equation (4)

$$Accuracy = \frac{TP + TN}{TP + TN + FP + FN}, \tag{4}$$

where *TP = True Positives, TN = True Negatives, FP = False Positives,* and *FN = False Negatives*. Table 6 shows an example confusion matrix (VGG16 Model – 50 epoch - Config. #9 – Test data) to calculate model's accuracy. The accuracy is 0.9429, or 94.29% (94 out of 100 instances yielded correct predictions) regarding equation 4.That indicates that our energy loss module classifier is very effective in detecting between *Matter* and *Matter-LBT*.

Table 6. Confusion Matrix for VGG16 Model – 50 epoch - Config. #9 – Test data

	Predicted	
	MATTER	MATTER-LBT
MATTER	TP: 56192	FP: 3039
MATTER-LBT	FN: 3808	TN: 56961

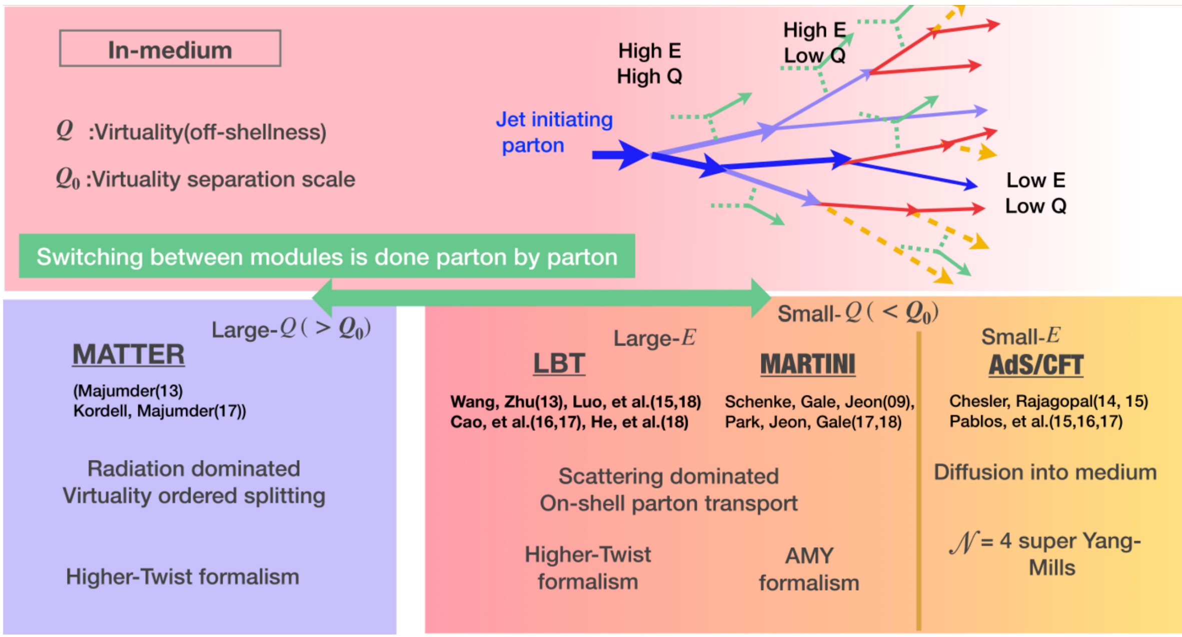

Figure 5. Multi-stage approach in heavy-ion collisions, credit to Y. Tachibana et. al. from JETSCAPE collaboration.

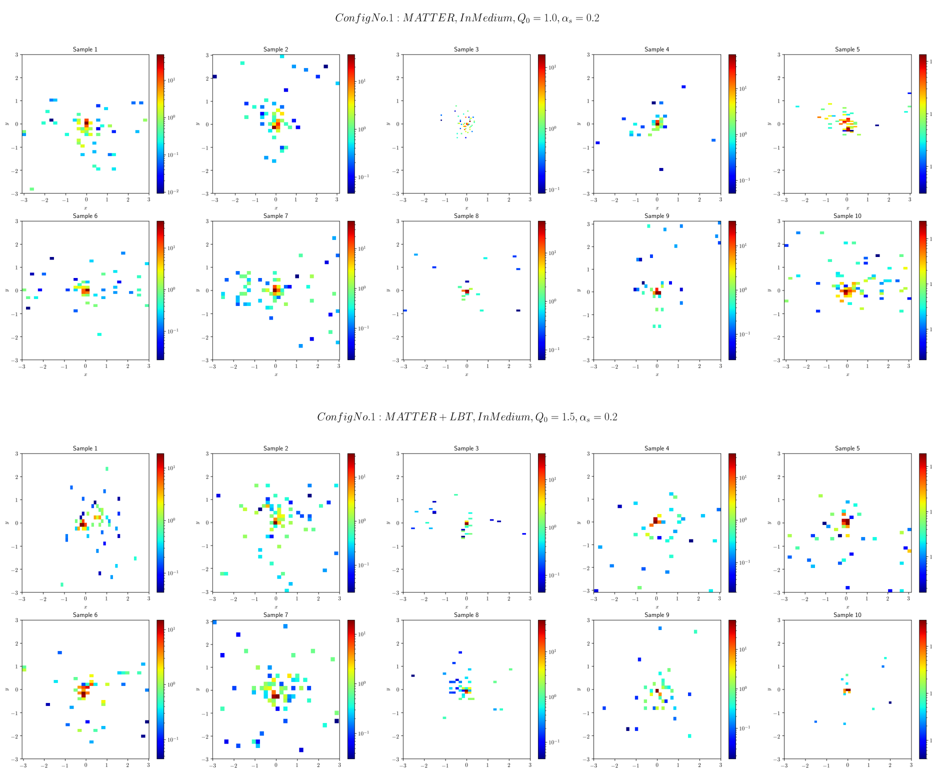

Figure 6. Dataset: Sample events: Config No. 1 Matter and Matter-LBT.

13. VGG16 Training for 30 epochs

In this appendix, we provide the detailed analysis for VGG16 traning for 30 epochs. Table 7 demonstrates the

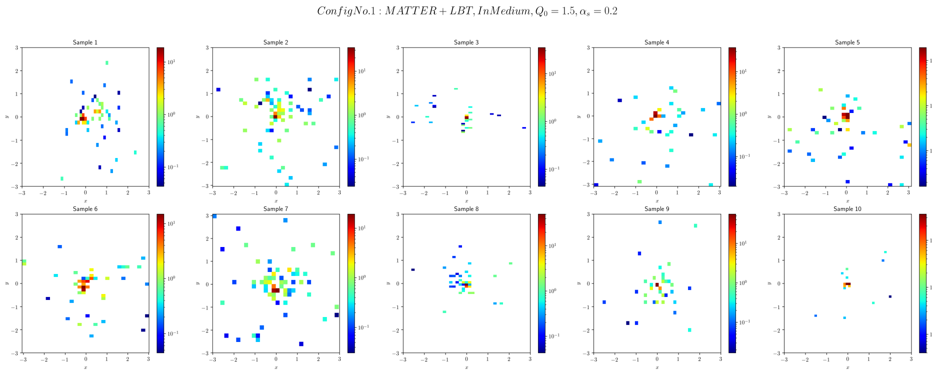

Figure 7. dataset: Sample events: Config No. 1 Matter-LBT.

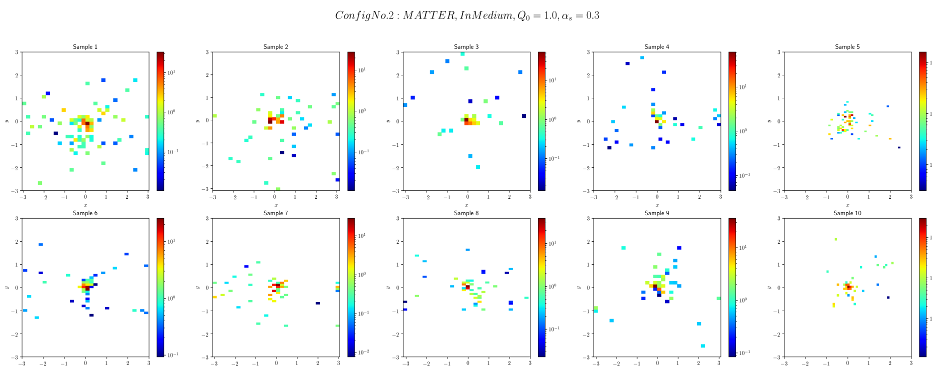

Figure 8. dataset: Sample events: Config No. 2 Matter.

Table 7. VGG16 model with 30 epochs: accuracy.

	Accuracy (%)		
	Train	Validation	Test
Config No. 1	89.395	89.4242	89.1383
Config No. 2	91.031	91.0596	91.5408
Config No. 3	84.5407	84.6833	84.4558
Config No. 4	76.0095	76.1054	75.9908
Config No. 5	91.7856	91.8829	91.6892
Config No. 6	94.367	94.3083	94.3483
Config No. 7	86.5311	86.41	86.2825
Config No. 8	93.029	93.0608	93.0133
Config No. 9	94.1714	94.1717	94.0925

loss and accuracy diagrams and table 8 demonstrates the accuracy for nine configurations.

14. Early stopping on VGG15 models

To prevent overfitting early stopping techniques has been applied on the training models. Table 9 shows a detailed accuracy report on each model when it confronted early stopping on VGG16 for 50 epochs.

15. Accuracy central tendency and variation for MNIST and VGG16 models

In this section, models' accruacy results with central tendency (mean) and their variation (error bars) in Figure 24.

15.1. Analysis of Machine Learning Models

In the pursuit of evaluating the efficacy and applicability of the ML-JET dataset, a series of experiments were conducted employing diverse machine learning methodologies. These encompassed logistic regression, decision trees, K-Nearest Neighbor (KNN), Support Vector Machine (SVM) including its linear variant (Linear SVC), and Random Forest, each deployed with various architectures and configurations. Training these models on the ML-JET dataset, we gauged their performance against a held-out test set.

Figure 3 illustrates the binary classification accuracy along with error bars for five distinct machine learning models trained over 5-fold cross-validation and employing four

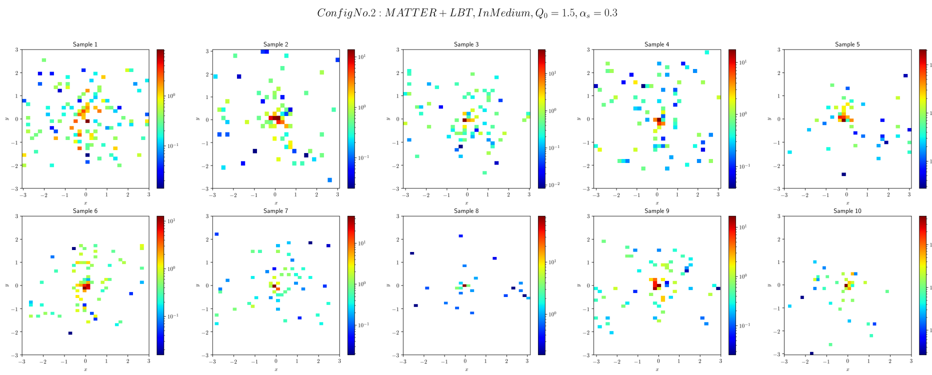

Figure 9. dataset: Sample events: Config No. 2 Matter-LBT.

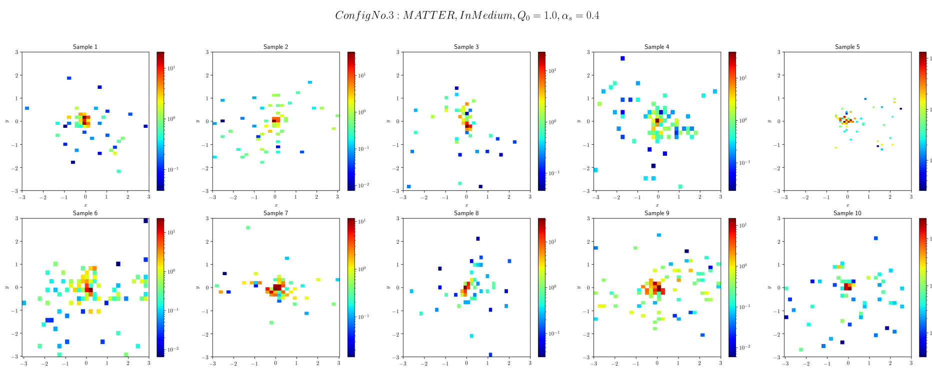

Figure 10. dataset: Sample events: Config No. 3 Matter.

variations in dataset size ranging from 1K to 1000K instances. Our findings underscore the ML-JET dataset's proficiency, particularly in logistic regression models for tasks pertaining to energy loss module classification. These models achieved an average accuracy of approximately 87%, surpassing the performance of other models. However, it's noteworthy that the accuracy of logistic regression models plateaued at around 87% even with an increase in dataset size from 10^5 to 10^6, prompting consideration for alternative approaches within deep learning paradigms.

Linear SVC, Random Forest, KNN, and Decision Tree techniques followed in rankings from 2 to 5 respectively, in terms of their accuracy performance. Similar to logistic regression, Linear SVC exhibited a plateauing trend in accuracy, albeit at around 80% on average. Random Forest displayed a linear increase in accuracy with the expansion of the dataset size. However, extrapolating this trend suggests an immense dataset size requirement of 10^{10} instances to merely attain logistic regression accuracy levels with a dataset size of 10^6. KNN and Random Forest exhibited analogous accuracy trends, showing improvements between 10^3 to 10^4 instances, with marginal gains thereafter, boasting approximately 2-3% better performance.

16. Analysis of Point Cloud Models

Upon scrutinizing the limitations of contemporary machine learning models in terms of computational capacity and accuracy, our focus shifted towards exploring cutting-edge deep neural network methodologies. Specifically, we delved into training PointNet [29] models for addressing the energy loss binary classification problem, employing various settings and configurations.

Figure 4a presents a comprehensive overview of the binary classification accuracy along with error bars for five distinct machine learning models, trained over 10 folds, 32 epochs, and with dataset sizes ranging from 1K to 1000K instances. The results obtained are highly encouraging. Notably, a linear correlation is observed between dataset size and average accuracy. Furthermore, as the dataset size increases, the standard deviation of accuracy diminishes, indicating improved stability in accuracy metrics. Notably, point clouds achieve an average accuracy of approximately 88% with a dataset size of 10^5. Remarkably, this outperforms logistic regression on a dataset size of 10^6, showcas-

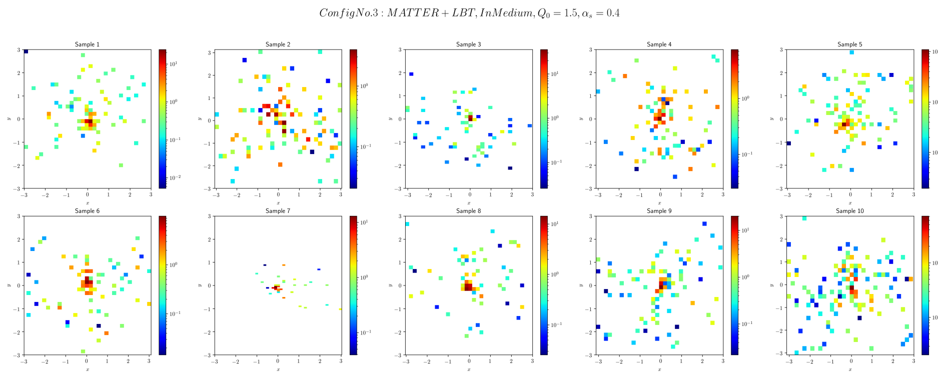

Figure 11. dataset: Sample events: Config No. 3 Matter-LBT.

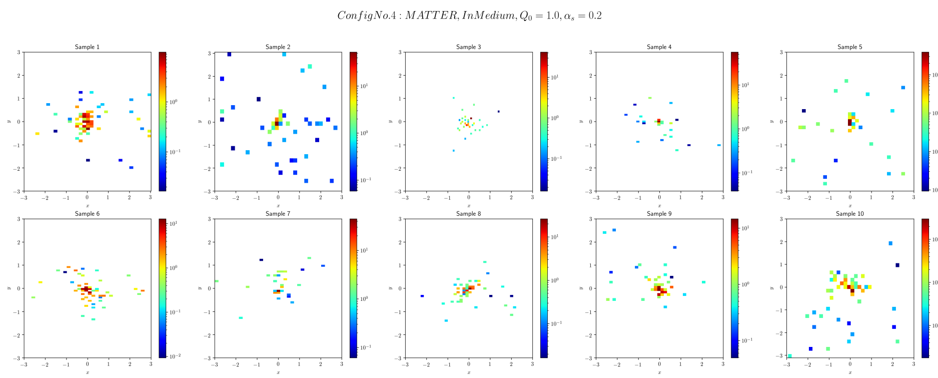

Figure 12. dataset: Sample events: Config No. 4 Matter.

ing the consistent and linear progress achieved by PointNet models.

Additionally, Figure 4b illustrates the trajectory of training loss across epochs, demonstrating a consistent decrease, indicating effective learning from the training data. Conversely, the validation loss exhibits an initial decrease but later manifests fluctuations, suggestive of potential overfitting as the training progresses. Towards the latter stages of training, a slight increase in validation loss further corroborates the presence of overfitting tendencies.

The training accuracy steadily ascends with each epoch, as anticipated due to the model's learning process. However, the validation accuracy showcases a plateauing trend after a certain epoch, indicating limited improvement in performance on unseen data beyond a certain point.

The widening chasm between training and validation loss serves as a telltale sign of overfitting, wherein the model excels on the training data but struggles to generalize to unseen instances. Despite these challenges, the final validation accuracy hovers around 86-87%, a commendable achievement within the realm of heavy ion physics and its specific requirements.

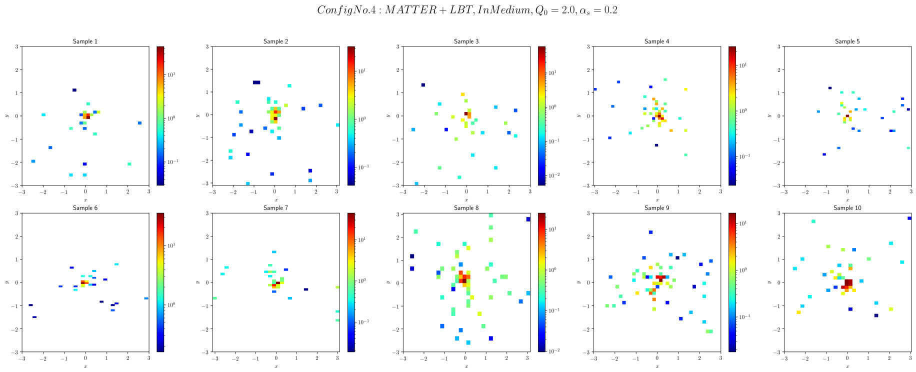

Figure 13. dataset: Sample events: Config No. 4 Matter-LBT.

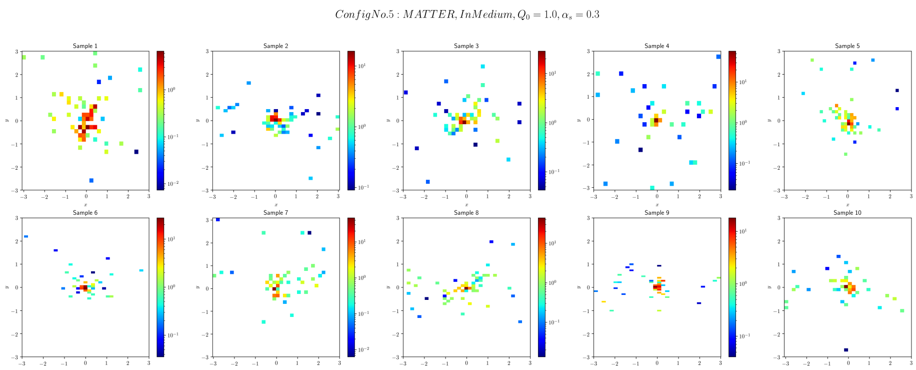

Figure 14. dataset: Sample events: Config No. 5 Matter.

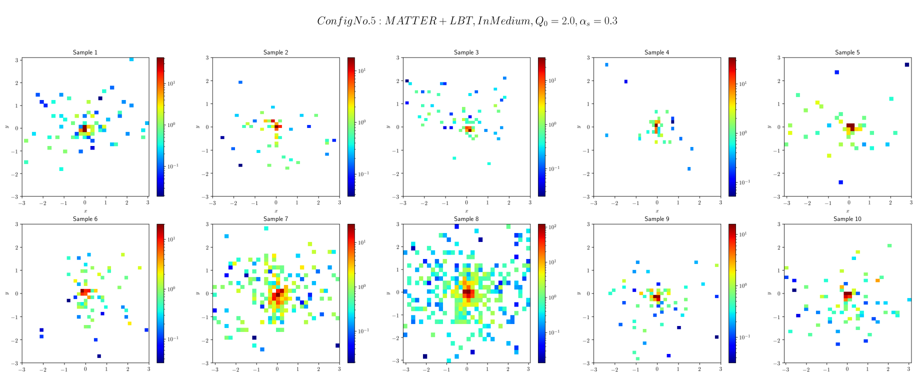

Figure 15. dataset: Sample events: Config No. 5 Matter-LBT.

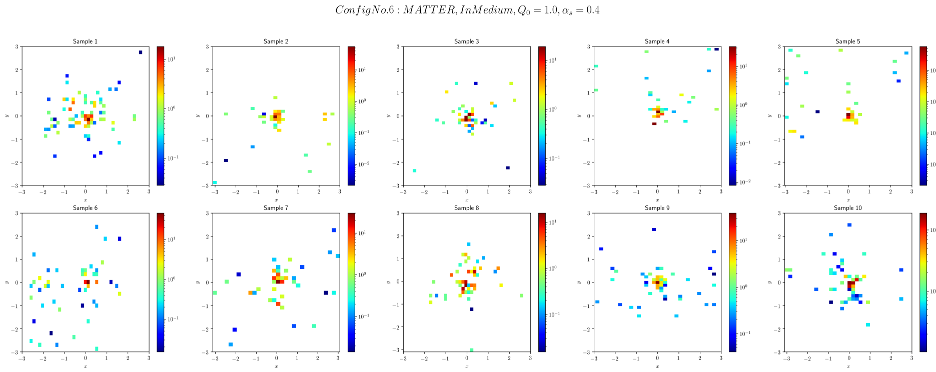

Figure 16. dataset: Sample events: Config No. 6 Matter.

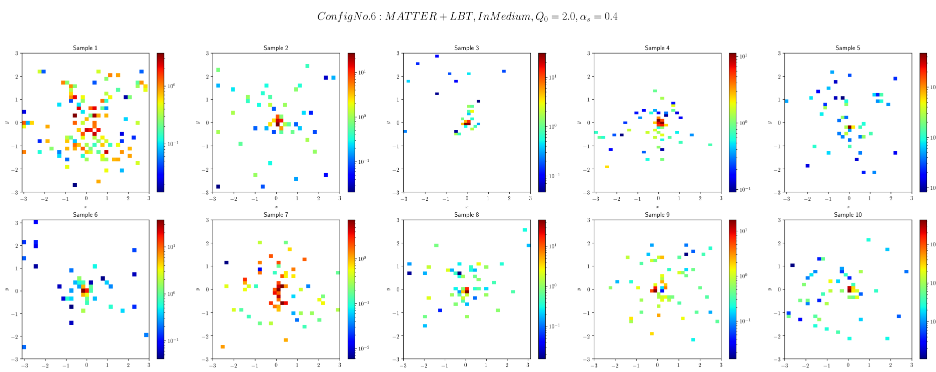

Figure 17. dataset: Sample events: Config No. 6 Matter-LBT.

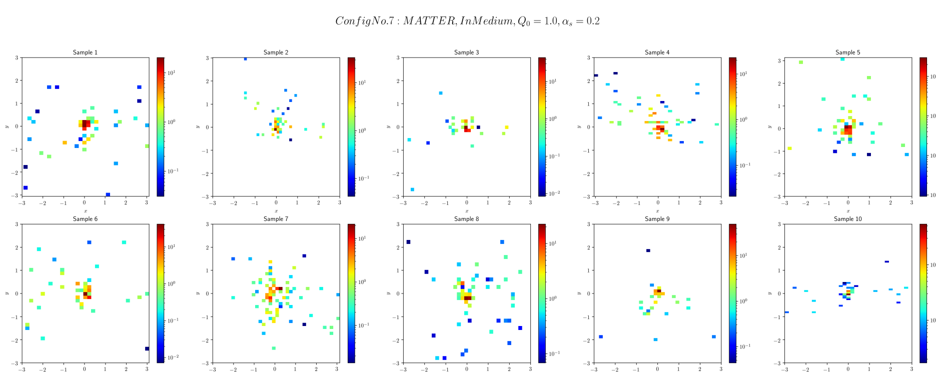

Figure 18. dataset: Sample events: Config No. 7 Matter.

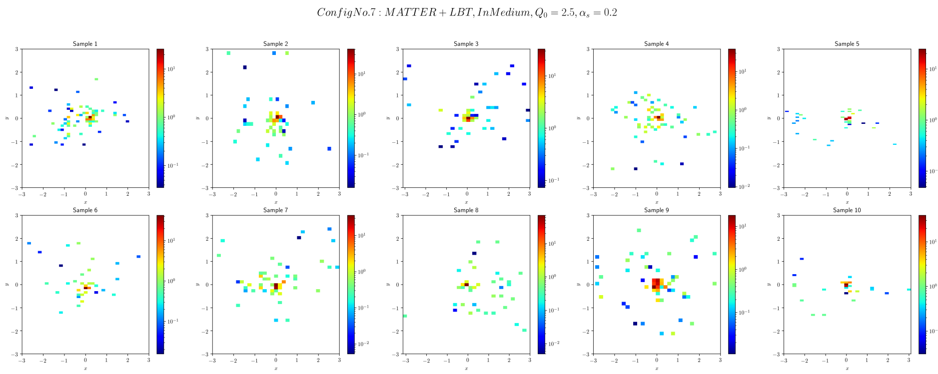

Figure 19. dataset: Sample events: Config No. 7 Matter-LBT.

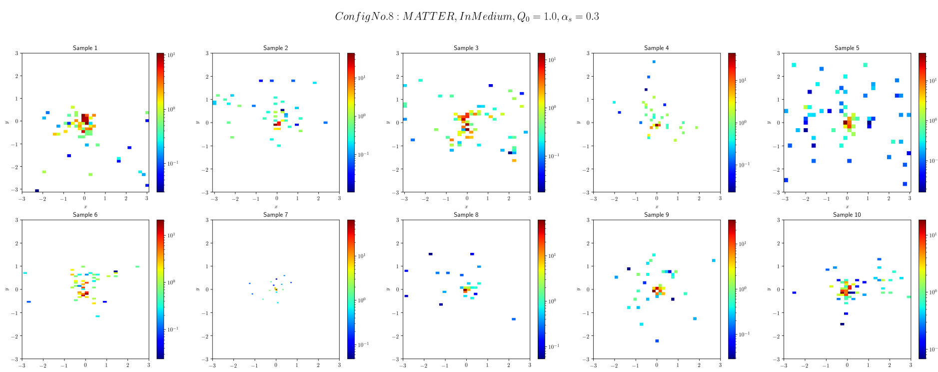

Figure 20. dataset: Sample events: Config No. 8 Matter.

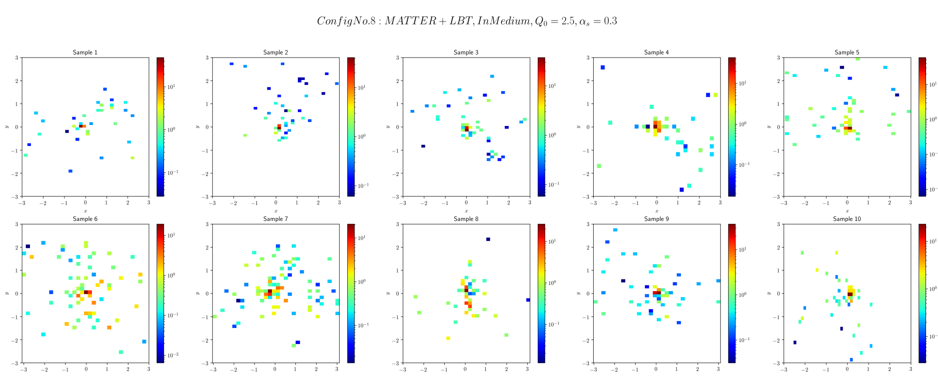

Figure 21. dataset: Sample events: Config No. 8 Matter-LBT.

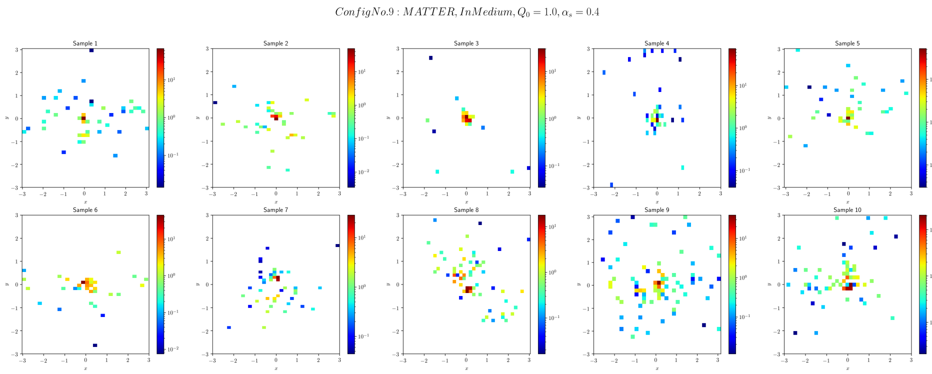

Figure 22. dataset: Sample events: Config No. 9 Matter.

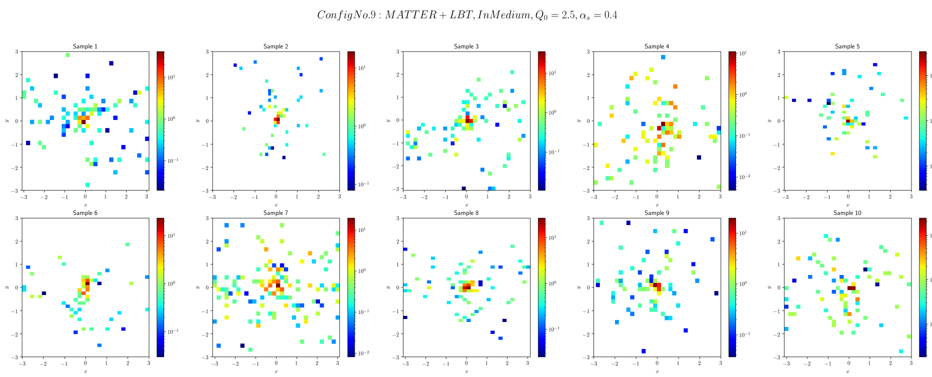

Figure 23. dataset: Sample events: Config No. 9 Matter-LBT.

Table 8. VGG16 model with 30 epochs: accuracy & loss diagrams.

	$\alpha_s = 0.2$	$\alpha_s = 0.3$	$\alpha_s = 0.4$
Matter: $q0 = 1$, Matter-LBT: $q0 = 1.5$.	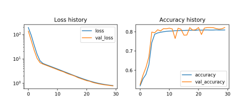	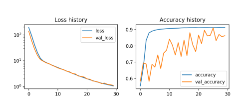	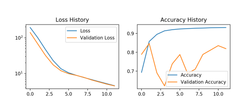
Matter: $q0 = 1$, Matter-LBT: $q0 = 2$.	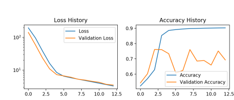	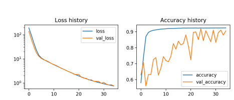	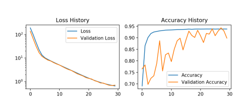
Matter: $q0 = 1$, Matter-LBT: $q0 = 2.5$.	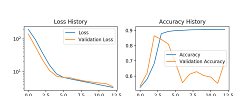	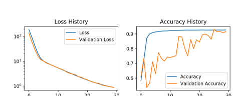	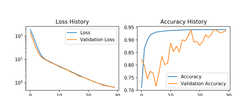

Table 9. VGG16 trained models for 50 epochs early stopping and their converged accuracy

Configuration No.	2	3	4	5	7	8
Accuracy (%)	92	93	90	93	89	93

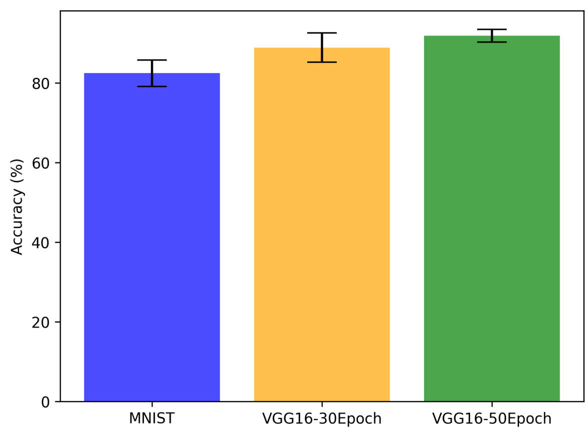

Figure 24. trained models accuracy mean and error bar.